

SEASONAL CYCLES IN AEROSOL OPTICAL THICKNESS IN TWO AUSTRALIAN CITIES

Zahra Bouya, Gail Box and Michael Box
School of Physics University of New South Wales, Sydney 2052, Australia

Abstract

In this study, we investigate the seasonal cycles in aerosol optical thickness in two Australian cities: Sydney and Darwin. We used multiyear optical thickness measurements, which permit an analysis of the seasonal variability. A regression analysis has been performed on 25 months data from the Sydney site to look for any seasonal cycles. We find a clear annual cycle, with amplitude approximately half the mean, with the highest aerosol loading occurring during summer months. We have also found a very clear annual cycle for the Angstrom coefficient, with the dominance of larger particles during the Australian autumn. A similar regression analysis was performed on the Darwin site from March 2002 to June 2003. It shows a strong seasonal cycle in aerosol optical depth and Angstrom coefficient with marked periods of low optical thickness and periods of high optical thickness. The maximum aerosol optical thickness coincides with the biomass-burning season in the north. During the course of this study we developed a simple way to introduce the temporal functional variation of the aerosol load.

Keywords: Aerosol, Optical thickness, Angstrom Coefficient, Cycle, Darwin, Sydney.

1. Introduction

Aerosols are tiny, suspended solid particles or liquid droplets that enter the atmosphere from either natural or human sources, such as forest fires or fossil fuel burning. Natural sources include volcanic eruptions, dust storms, ocean waves, and forest fires. Industrial anthropogenic sources include power plants, oil refineries, and other manufacturers. Aerosols influence climate directly by reflection of the incoming solar radiation, and indirectly by modifying cloud properties.

This paper summarizes the characterization of the aerosol seasonality in two Australian cities carried out using a combination of MFRSR measurements from Darwin and Sydney. The data used for Darwin site was collected from the Tropical Western Pacific (TWP) facilities site implemented by the U.S. Department of Energy (DOE) Atmospheric Radiation Measurement (ARM) Program. The Darwin site is located at 12.42 S, 130.81 W, altitude 23.89 m. The data used for Sydney were obtained from the ground-based measurements by the MFRSR installed at the Kensington campus of University of New South Wales, Sydney at 33.9 S and 151.2 E at 85 m above the sea level. Optical thickness measurements were taken at Sydney site from

December 1995 to February 1998 and from Darwin from March 2002 to June 2003.

The first section summarizes the methodology used to derive the aerosol optical thickness from the radiometer readings, the second section examines the seasonal cycles of aerosol optical thickness and Angstrom coefficient in both cities. The final section is a summary of the aerosol optical thickness seasonality in both Darwin and Sydney and a comparison of the cycles in the two cities.

2. Methodology

The raw data that the MFRSR collects are voltage counts, which are calibrated by the host software into spectral irradiances (Watts per sq. metre per micron). The total optical depth is computed through a Langley analysis, and calculations can be done to derive other data such as aerosol optical depth, ozone abundance and water vapor. The direct solar beam is attenuated according to the Beer-Bouguer-Lambert law as it passes through our atmosphere,

$$I = I_0 e^{-m \cdot \tau} \quad (1)$$

where m is the airmass factor which describes the enhancement of the slant path over the vertical and τ is the vertical optical depth of the atmosphere.

The airmass factor can be determined from the solar zenith angle (which is a function of latitude, season, and time of day). If SZA represents the solar zenith angle, then the airmass factor is, $m = [\cos(\text{SZA})]^{-1}$, as long as the sun is fairly high in the sky. Otherwise, a modified expression should be used which accounts for the sphericity of the Earth,

$$m = [\cos(\text{SZA}) + 0.50572(1.46468 - \text{SZA})^{-1.6364}]^{-1},$$

where SZA is in radians (Harrison and Michalsky 1994; Kasten 1966).

Taking the natural logarithm of both sides of Eqn.1 gives:

$$\ln(I) = \ln(I_0) - \tau \cdot m$$

which is of the form $y = a + bx$ such that $a = \ln(I_0)$ represents the y -intercept and $b = \tau$ represents the slope. Thus, if the m is plotted versus the logarithm of the irradiance (at a given wavelength) for many data points throughout a morning or afternoon, a straight line should result. Linear regression performed on this data will give the intercept and slope, which amount to the logarithm of the extra-terrestrial irradiance and the vertical optical depth, respectively.

The vertical optical depth of the atmosphere includes components from molecular and aerosol scattering and, depending on the channel, may also include absorption by ozone or water vapor. The aerosol optical depth is calculated through,

$$\tau_{\text{aer}} = \tau_{\text{total}} - (\tau_{\text{ray}} + \tau_{\text{O}_3} + \tau_{\text{H}_2\text{O}})$$

Ozone abundance may be inferred by measurements made by the 500, 615, and 673 nm channels. These wavelengths, particularly the 615 and 673 nm wavelengths, are influenced by the Chappuis band of ozone (Goody and Yung 1989). Water vapor primarily affects the 940 nm channel. (We have ignored this channel in this work.) Rayleigh scattering most strongly affects the lower wavelength channels. This phenomenon is well understood, and therefore can be removed from an analysis of the optical depth measurements made at all wavelengths. The Rayleigh optical depth can be calculated based solely on the pressure of the measurement site, P , using,

$$\tau_{\text{ray}} = 0.008569\lambda^{-4}(1 + 0.0113\lambda^{-2} + 0.00013\lambda^{-4}) P/P_0$$

where $P_0 = 1013.25$ hPa is standard surface pressure and λ is the wavelength in nm (Hansen and Travis, 1974). Rayleigh scattering is well understood and its total contribution to the optical depth can be easily removed. The ozone is removed using a technique outlined by Box and Taha (1999). Once Rayleigh scattering and ozone

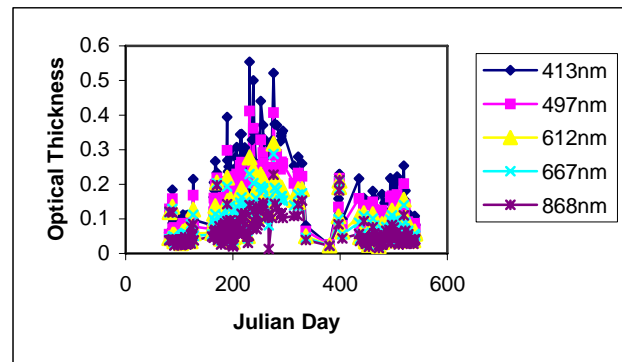
effects are calculated, subtracting them from the total optical depth results in aerosol optical depth.

3. Seasonal Cycle in aerosol optical thickness and Angstrom coefficient

3.1. Darwin

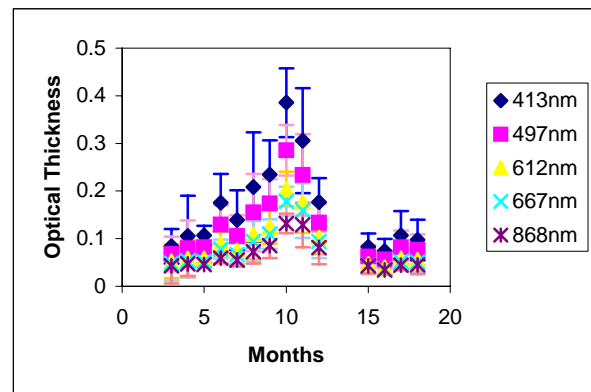
3.1.1. Aerosol optical thickness

The time series of atmospheric aerosol measurements obtained from Darwin site in Northern Territory of Australia during 2002 and



2003 is shown in Figure.1.

Figure 1. Temporal variation of aerosol



optical thickness for Darwin

Figure 2. Monthly mean optical depth for Darwin.

The monthly mean and standard deviation of the aerosol optical depth data is shown in Figure 2. The aerosol optical depth monthly average shows seasonality, with marked periods of low optical depth during the season March-May, while periods of high optical depth is associated with the spring season September-November coinciding with maximum burning in the north (Vanderzalm et al,

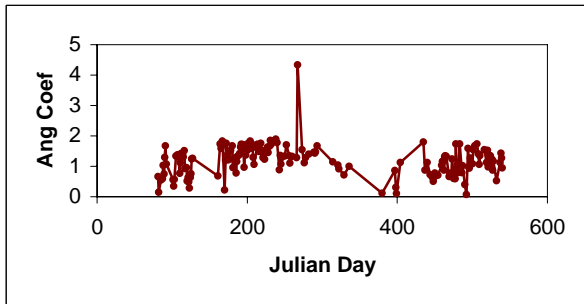
2003). The same seasonality is observed for all the wavelengths.

3.1.2 Angstrom coefficient

Of particular interest is the Angstrom exponent, or "beta" parameter. This parameter derived from the equation (Ångstrom 1926):

$$\tau = c \cdot \lambda^{-\beta}$$

is indicative of an aerosol's size and other physical characteristics. Beta was calculated for each stable



day and its daily value ranges from 0.08 to 1.90, with one day (September 24, 2002) with very high value (4.218). This high Angstrom Coefficient is probably due to forest fires in the vicinity of the Darwin area at this time or some other distinct mechanism of aerosol formation (Figure 3).

Figure 3. Daily variation of the Angstrom coefficient in Darwin.

The monthly average of the Angstrom coefficient shows seasonality. There are marked periods of low Angstrom coefficient during the wet season (December-March) caused by the dominance of large particles, while periods of high Angstrom coefficient are associated with the peak of the burning season August-October, when small smoke particles dominate (Figure 4)

Figure 4. Monthly mean of the Angstrom coefficient form March 2002 to June 2003.

3.1.3. Regression fit

More information regarding the seasonal cycle of

the aerosol optical thickness and Angstrom coefficient appears when a regression fit is performed to the 15 months data. To investigate any trends and cycles that the data may contain, we have chosen to fit each data set with the regression function:

$$\tau(t) = m_0 + \alpha \cos(2\pi(m_1 \frac{t}{12} + \phi))$$

where t is the time in months starting from March 2002 (t = 0) and m₀, m₁, α and φ are fitting parameters. An annual cycle for the aerosol optical depth and Angstrom coefficient of 12 months was observed over Darwin. The seasonal cycles of aerosol optical depth at all wavelengths are remarkably coherent. The optical thickness at all 5 wavelengths shows the same seasonality with marked periods of low optical thickness during the period March-May while periods of high optical thickness occur in the period September-November. The maximum aerosol load occurs in October for all the wavelengths and the parameter m₁ = 1 (Table 1) is consistent for all the wavelengths. Figure 5 (λ = 413 nm) shows an example of the trends while Table 1 show the fitting parameter values and standard error. We also fitted the Angstrom coefficient with the same function, Figure 6, which shows an annual cycle with m₁ = 1. We have included the fitting parameters in Table 1

Fig.5. Aerosol optical thickness time series

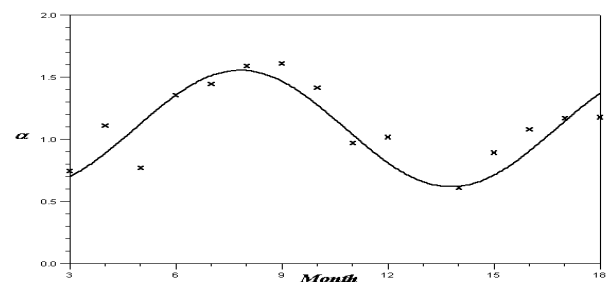
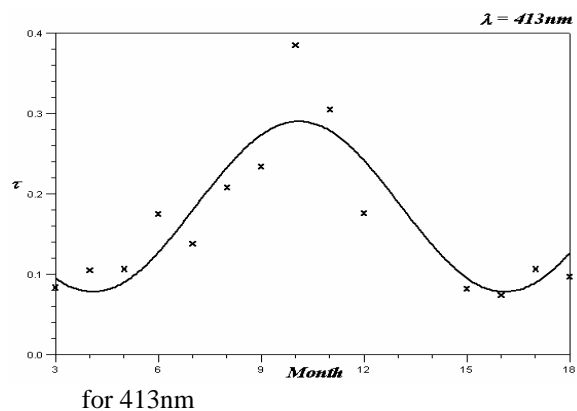


Fig.6. Time series of the Angstrom coefficient

Table.1 Fitting parameter values for the aerosol cycles

λ (nm)	m_0		m_1		α		ρ	
	Value	St. Err.	Value	St. Err.	Value	St. Err.	Value	St. Err.
413	0.184	0.013	0.998	0.033	0.106	0.016	0.160	0.030
497	0.139	0.009	1.001	0.032	0.078	0.012	0.157	0.030
612	0.102	0.007	1.001	0.032	0.057	0.008	0.147	0.029
667	0.091	0.006	1.002	0.031	0.050	0.007	0.140	0.028
868	0.074	0.004	1.004	0.029	0.036	0.005	0.123	0.020
Ang Coeff.	1.088	0.056	1.006	0.026	0.467	0.080	0.344	0.027

3.2. Sydney

3.2.1 Aerosol optical thickness

In this section we examine the aerosol seasonal behaviour over Sydney. The data were obtained from the ground-based irradiance measurements by the MFRSR operated at the Kensington campus of the University of New South Wales from December 1995 to February 1998. Figure 7 illustrates the day to day variability of aerosol optical thickness.

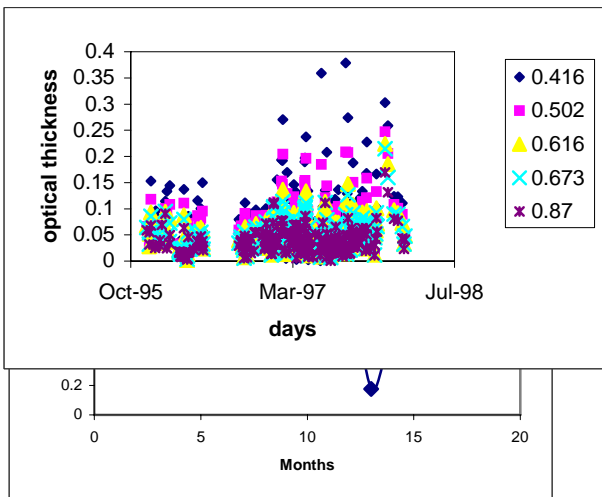
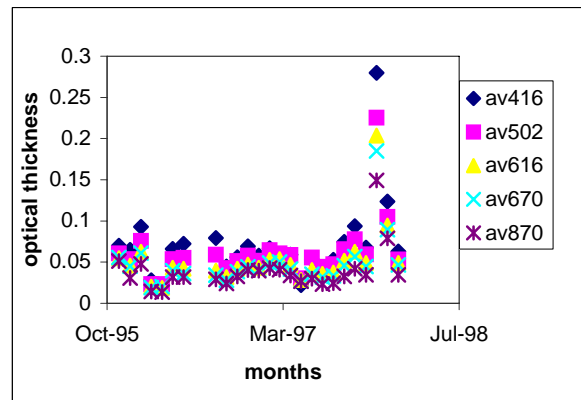


Figure 7. Temporal variation of aerosol optical thickness from December 1995 to February 1998 in Sydney.

The monthly mean aerosol optical thickness for all 5 wavelength is presented in Figure 8. The aerosol optical depth shows seasonality, with marked periods of high optical depth during the season November-January afternoon, while period of low optical depth is associated with the season

May-July. The same seasonality is observed for all the wavelengths. Again we have fitted each data



set with same periodic function. The time series of aerosol optical thickness for the wavelength 502 nm is shown in Figure 9. The seasonal cycle and the time series of aerosol optical depth at all the 5 wavelengths is clearly evident. The shape of the seasonal cycle is roughly the same for all the wavelengths.

Figure 8. Monthly mean aerosol optical thickness from December 1995 to February 1998 in Sydney.

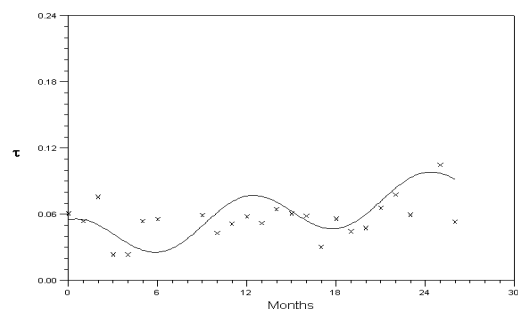


Figure 9. Aerosol optical thickness time series for 502nm, Sydney

3.2.2 Angstrom coefficient

The annual cycle of the Angstrom coefficient displays a minimum during Australian summer and a significant increase toward the Australian spring season with a maximum during September. As a confirmation of this signature we show below the seasonal cycle of the Angstrom coefficient. As shown in Figure 10 we have fitted the same functional form as the aerosol optical thickness; the monthly mean shows a clear seasonal cycle.

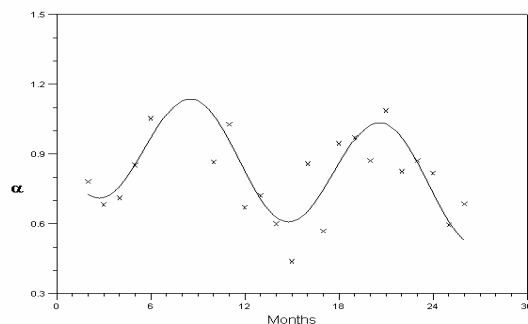


Figure 10. Angstrom coefficient time series for Sydney.

4. Conclusion

The seasonal cycle of aerosol loading in Sydney and Darwin is remarkably strong. The aerosol optical thickness and Angstrom coefficient have been fitted with the same functional form. There is a difference in the time of occurrence of the maximum load: for Darwin, the maximum load occurs in October which is when biomass burning occurs in the Northern Territory, whereas the maximum optical thickness in Sydney occurs in January. According to the Bureau of Meteorology data base (<http://www.bom.gov/info/leaflets/>) the bushfire season occurs in Darwin during winter and spring, and in Sydney in spring and late summer. In Sydney, the maximum aerosol load occurs in

January and may be associated with bushfires, however in a large industrial city such as Sydney, there are obviously other factors. The period of the cycle, one year, is consistent for the two locations and time periods, but there is a difference in the other fitting parameters, which reflects the differences in the aerosols in the two cities.

Acknowledgments

We would like to thank the ARM Archive for providing with the radiometer data and giving us the opportunity to study the trend in the Northern Territory of Australia. We would like to thank Ghassan Taha and Maja Kuzmanoski for processing some of the Sydney data.

References

- Ångström A., 1929. 'On the atmospheric transmission of sun radiation and on dust in the air', *Gerg. Ann.*, **11**, 156-166.
- Bureau of Meteorology, http://www.bom.gov.au/info/leaflets/bushfire_weather.pdf
- Goody R. M. and Yung Y. L. 1989. *Atmospheric Radiation; Theoretical Basis*. Oxford U. P.
- Hansen J. E. and Travis L. D. 1974. 'Light scattering in planetary atmospheres', *Space Sci. Rev.* **16**, 527-610.
- Harrison, L. and Michalsky, J., 1994. 'Objective algorithms for the retrieval of optical depths from ground instruments', *Applied Optics* **33**, 5126-5132.
- Kasten, F., 1966. 'A new table and approximation formula for relative air mass', *Arch. Meteorol. Geophys. Bioklimatol. Ser.B* **14**, 206-223.
- Taha G. and Box G. P. 1999. 'New Method for inferring total ozone', *Geophysical Research Letters*, **26**, 3085-3088.
- Vanderzalm J. L. et al., 2003. 'Impact of Seasonal Biomass Burning in the 'Top End' of Regional Northern Australia' *Clean Air (Aust.)*. **37**, 28-34.